Journal of Inflammation Research

Dovepress
Taylor & Francis Group

Open Access Full Text Article

ORIGINAL RESEARCH

Xianglian Anchang Decoction Mitigates Ulcerative Colitis via Inhibition of TLR-4-Mediated Pyroptosis

Shixiong Zhang[1,2,*], Yuhua Wang[1,*], Xuetong Ren[1,*], Haoyu Chen[1,*], Tianyu Gao[1], Yang Liu[1], Lishan Lu[1], Junzhuo Ma[1], Haiyan Bai[1,2], Yangang Wang[1,3]

[1]Graduate School, Hebei University of Chinese Medicine, Shijiazhuang, Hebei, People's Republic of China; [2]The First Affiliated Hospital of Hebei University of Chinese Medicine, Hebei University of Chinese Medicine, Shijiazhuang, Hebei, People's Republic of China; [3]The Third Affiliated Hospital of Beijing University of Chinese Medicine, Beijing University of Chinese Medicine, Beijing, People's Republic of China

*These authors contributed equally to this work

Correspondence: Yangang Wang; Haiyan Bai, Email piwei001@163.com; bhyan@2008.sina.com

Background: Xianglian Anchang Decoction (XLAC) shows significant promise in treating ulcerative colitis (UC) based on clinical experience. However, the specific mechanism of XLAC treatment for UC is still not well understood.

Purpose: This study aims to explore the pharmacological mechanism of XLAC in treating UC through network pharmacology and experimental verification.

Methods: In this study, DSS-induced UC mouse model was established to evaluate the effects of XLAC on body weight, Disease Activity Index scores, spleen index, and colon length. Pathological change and intestinal barrier integrity were analyzed via hematoxylin-eosin, periodic acid-Schiff staining, immunofluorescence, RT-qPCR, Western blot, and ELISA. Network pharmacology and bioinformatics analyses were employed to predict potential targets of XLAC, followed by molecular docking to validate the binding affinity between key components and TLR4.

Results: XLAC significantly ameliorated weight loss, colon shortening, and splenomegaly in UC mice ($P < 0.001$), restored intestinal barrier integrity, and increased the expression of tight junction proteins (ZO-1/Occludin) and goblet cell numbers. Network pharmacology identified TLR4 as a key target, and molecular docking demonstrated strong binding affinity (Vina score < -5) between XLAC active components (eg, trans-4-coumaric acid, methyl cinnamate) and TLR4. In vivo experiments confirmed that XLAC downregulated the protein levels of TLR4, NLRP3, and GSDMD-N, as well as the mRNA expression of IL-1β and IL-18 ($P < 0.05$), thereby suppressing pyroptosis.

Conclusion: XLAC alleviates UC inflammation and intestinal barrier damage by targeting TLR4 to inhibit NLRP3 inflammasome activation and GSDMD-mediated pyroptosis. This study provides mechanistic insights into the clinical efficacy of XLAC for UC treatment.

Keywords: Xianglian Anchang decoction, ulcerative colitis, TLR4, NLRP3, pyroptosis

Introduction

Ulcerative colitis (UC) is a non-specific inflammatory disease characterized by chronic inflammation or ulceration of the rectal and colonic mucosa.[1] Globally recognized as one of the most challenging intestinal disorders, UC represents a significant risk factor for colorectal cancer development.[2,3] The ongoing global industrialization process has induced adverse transformations in living habits and nutritional behaviors, consequently driving a significant epidemiological escalation in both the incidence and population prevalence of UC.[4,5] Current therapeutic approaches for UC continue to face significant challenges, including suboptimal response rates, high relapse incidence, and notable adverse effects.[6] Traditional Chinese Medicine (TCM) has garnered substantial attention in UC management due to its demonstrated safety and therapeutic efficacy. Accumulating evidence has established TCM as one of the most promising therapeutic

Received: 28 May 2025
Accepted: 25 August 2025
Published: 4 September 2025

Graphical Abstract

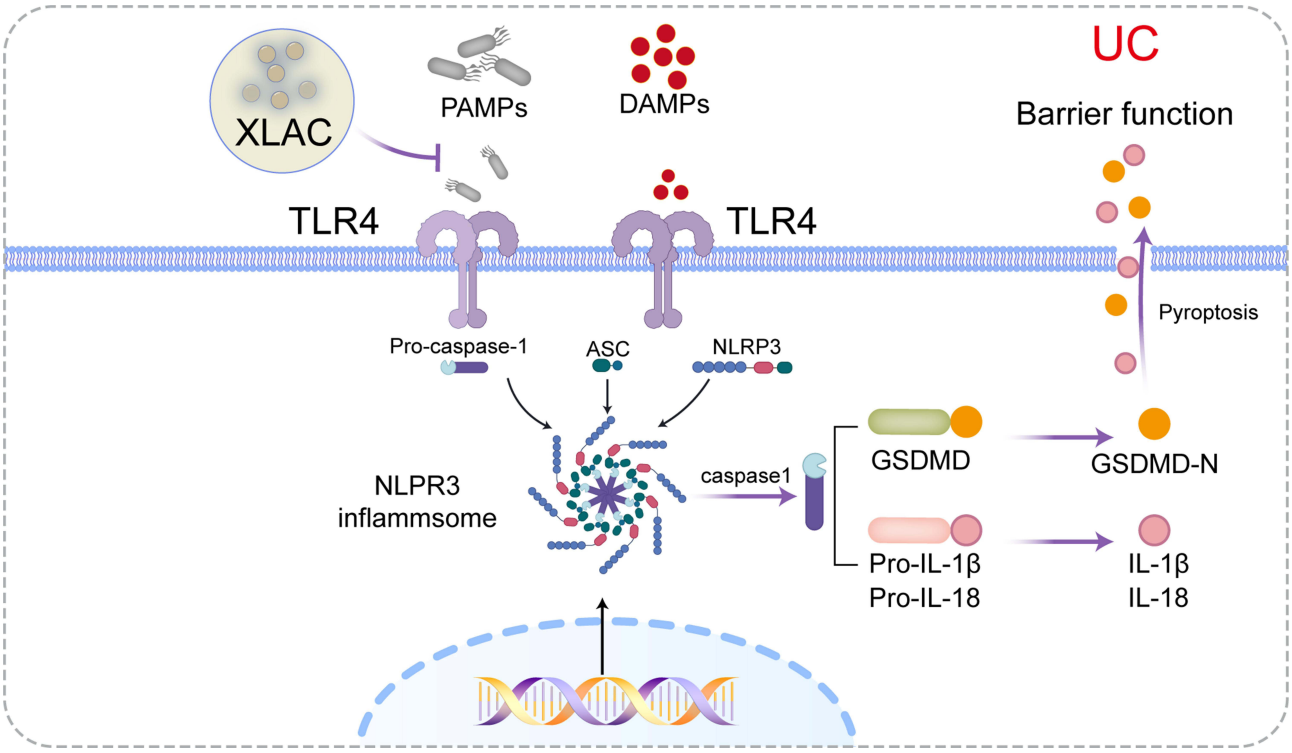

modalities for UC, exhibiting distinct advantages in disease stabilization, symptom amelioration, relapse prevention, and quality-of-life improvement, with interventions encompassing both single herbs and compound formulations.[7] Xianglian Anchang Decoction (XLAC) is a polyherbal formulation composed of 15 medicinal components: *Paeonia lactiflora* Pall. (Baishao), *Angelica dahurica* (Baizhi), *Plantago asiatica* L. (Cheqianzi), *Saposhnikovia divaricata* (Fangfeng), *Poria cocos* (Fuling), *Pueraria lobata* (Gegen), *Aspergillus oryzae* (Shenqu), *Lonicera japonica* Thunb. (Jinyinhua), *Aucklandia lappa* Decne. (Muxiang), *Panax notoginseng* (Sanqi), *Agrimonia pilosa* Ledeb. (Xianhecao), *Cynanchum paniculatum* (Xuchangqing), *Corydalis yanhusuo* W.T.Wang (Yanhusuo), *Scutellaria baicalensis* Georgi (Huangqin), and *Coptis chinensis* Franch. (Huanglian). XLAC is derived from Xianglian Wan, a classical formula first documented in the Ming Dynasty medical text Taiping Huimin Heji Ju Fang. To address the chronicity and complexity of UC, XLAC has expanded Xianglian Pill through evidence-based modifications while retaining the core components. And this herbal decoction has demonstrated significant efficacy in alleviating UC, although its exact mechanisms of action remain incompletely understood.

The pathogenesis of UC involves multiple interrelated factors: intestinal microbiota dysbiosis,[8,9] intestinal immune dysregulation,[10,11] mucosal homeostasis disruption,[12,13] and intestinal barrier dysfunction.[14,15] Notably, intestinal barrier dysfunction plays a pivotal role in UC pathogenesis, exhibiting a bidirectional "cause-effect cycle" characteristic.[16] Upon initiation of intestinal inflammation, compromised intestinal epithelial cells facilitate exposure of luminal noxious substances to the immune system, thereby triggering and amplifying inflammatory cascades. Consequently, elucidating the molecular mechanisms underlying intestinal epithelial cell injury may provide novel therapeutic targets for UC pathogenesis research.

Increased epithelial cell death is one of the hallmarks of UC and is positively correlated with the severity of inflammation.[17] Studies have found that inhibiting pyroptosis signaling can alleviate UC.[18] Pyroptosis is a form of programmed cell death triggered by inflammasomes, characterized by the continuous swelling of cells until the cell

membrane ruptures, leading to the release of cellular contents and thus causing a strong inflammatory response.[19] Appropriate pyroptosis is an important innate immune response of the body and plays a significant role in resisting infections, while excessive pyroptosis activity is highly pro-inflammatory and can lead to tissue damage.[20] TLR4 is a key member of the Toll-like receptor family, playing a crucial role in innate immune responses, especially in recognizing bacterial infections and triggering inflammatory responses.[21] TLR4 can lead to the activation of the NLRP3 inflammasome, promoting pyroptosis. During pyroptosis, pro-inflammatory factors such as IL-1β, IL-18, and a large number of additional danger signals and intracellular antigens are excessively released through pores formed by Gasdermin proteins, thereby exacerbating the inflammatory response and intestinal mucosal damage.[22]

In this study, we employed network pharmacology and bioinformatics approaches to investigate the molecular targets of XLAC in the treatment of UC, revealing that TLR4 plays a critical role in this process, which was preliminarily validated by molecular docking. Subsequent in vivo experiments further confirmed the essential role of TLR4 in XLAC's therapeutic effects on UC. These findings are expected to provide a theoretical foundation for the clinical efficacy of XLAC in UC treatment.

Materials and Methods

Experimental Animals

Fifty 8-week-old male C57BL/6J mice were purchased from Beijing Huafukang Bio-Technology Co., Ltd. (Beijing, China), with a certificate number SCXK (Jing) 2024–0003. The experimental animals were housed in a specific pathogen-free facility, maintained under constant temperature (25±0.5°C) and humidity (50±5%), with a 12-hour light/dark cycle, and provided with standard food. This experiment was approved by the Experimental Ethics Review Committee of the First Affiliated Hospital of Hebei University of Chinese Medicine (approval number: IACUC-HPHCM-2024078).

Preparation of XLAC

The XLAC was composed of 15 medicinal components. All crude drugs were obtained from the First Affiliated Hospital of Hebei University of Chinese Medicine (batch-certified). Following human-to-mouse dose conversion (9.1×clinical equivalent), two treatment concentrations were prepared: 1.24 g/mL (XLAC-L) and 2.48 g/mL (XLAC-H) through standardized extraction involving 1:10 (w/v) aqueous soaking, dual-cycle atmospheric-pressure extraction (1 h post-boiling), vacuum concentration at 70°C, and 4°C storage. The prepared extracts were administered via gavage for 7 consecutive days in subsequent experiments, with quality parameters including Latin nomenclature verification, extraction yield monitoring (68±3%), and HPLC fingerprinting validation to ensure batch consistency.

Experimental Procedure

Fifty C57BL/6J male mice were randomly divided into control group (n=10) and model group (n=40). After one week of adaptive feeding, the model group was administered 2% (w/v) DSS (molecular weight, 36–50 kDa; MP Biomedicals, Santa Ana, CA, United States) in drinking water to induce acute UC. Concurrently with the modeling, drug intervention was initiated, and the model group was randomly divided into four groups: the Model group, XLAC low-dose group (XLAC-L, 12.4g/kg), XLAC high-dose group (XLAC-H, 24.8g/kg), and the sulfasalazine group (SASP, 5g/kg). The Control group and Model group were gavage-fed an equal volume of distilled water. Intervene once a day for a total of 7 days. During the experiment, the general condition and body weight of the mice were observed daily. After the last administration, the mice were fasted for 24 hours without restriction of water. The mice were then anesthetized with 3% pentobarbital (45mg/kg) via intraperitoneal injection, followed by eyeball bleeding. After centrifugation, the serum was separated. The colon and spleen were collected, and the samples were frozen in liquid nitrogen and stored at −80°C or fixed in a 10% (w/v) formalin solution. In this study the colon length and spleen weight were measured. The overall experimental procedure was shown in Figure 1A.

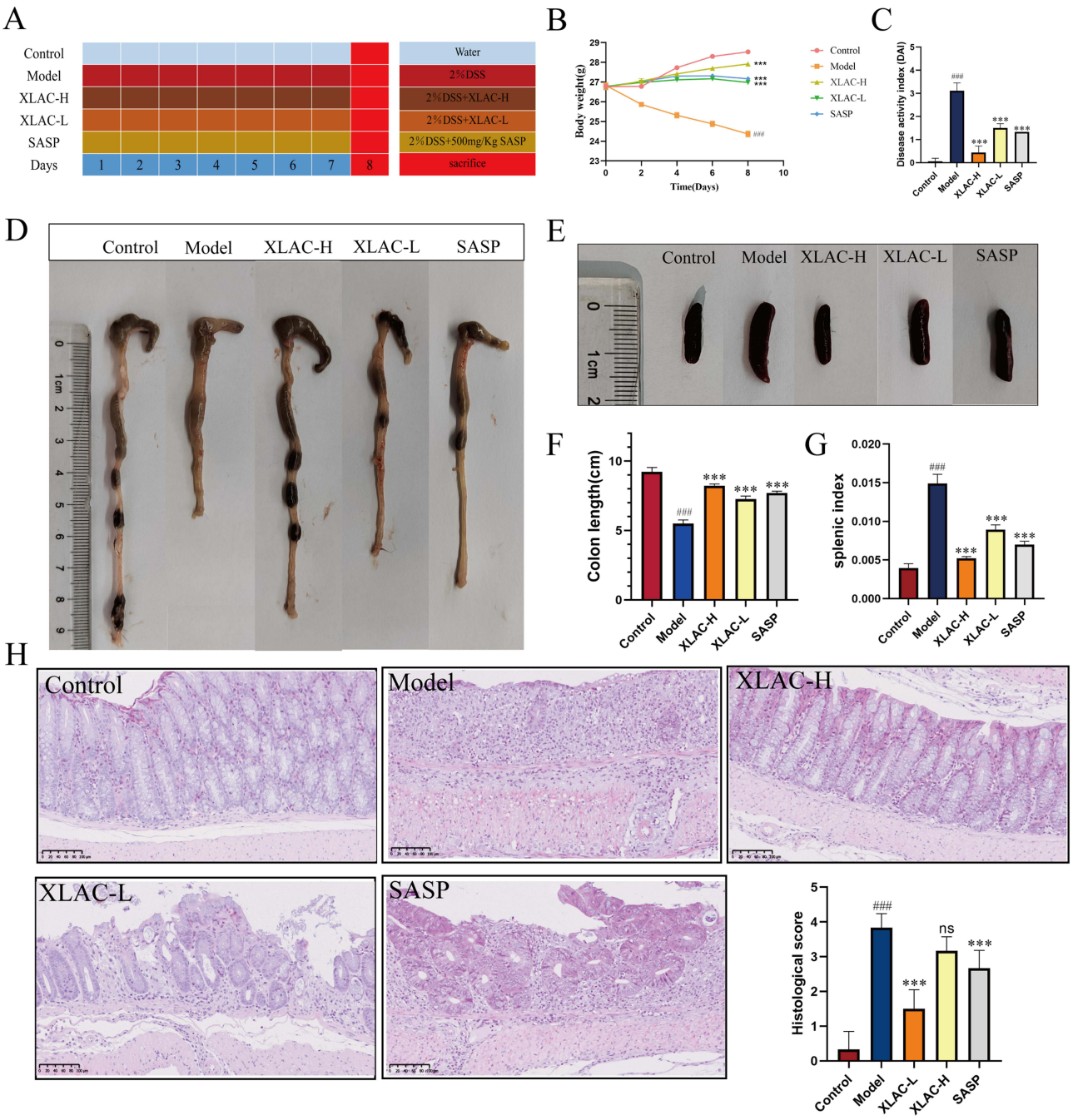

Figure 1 Beneficial effect of XLAC on intestinal inflammation in UC Mice. (**A**) Timeline of DSS administration and different treatments in mice. (**B**) Body weight change. (**C**) Disease activity index. (**D**) Representative images of colon length from each group. (**E**) Representative images of spleen from each group. (**F**) Comparison results of colon length for each group. (**G**) Comparison results of splenic index for each group (**H**) Results of HE staining (200×). The data were denoted as the mean ± SD (n = 6). ###P<0.001, compared to Control group; ***P<0.001, compared to Model group. ns represents no statistical difference.

Disease Activity Index (DAI) Scoring

Weight loss, stool consistency, and degree of intestinal bleeding were recorded daily in mice, and the DAI score was used to assess disease activity.[23] The DAI = (body weight loss score + stool consistency score + stool occult blood score) divided by 3.

Hematoxylin and Eosin Staining (H&E)

H&E staining was performed to observe histological changes in the colon tissue. The colon tissues were immersed in 4% paraformaldehyde for 24 hours and then embedded in paraffin blocks. Subsequently, the paraffin-embedded tissues were sectioned into 4 μm thick slices, deparaffinized using xylene, dehydrated through a graded series of alcohol, and stained with Hematoxylin and Eosin. The histopathological score of gastric mucosa was obtained by observing the degree of inflammatory infiltration and colonic mucosal damage under an optical microscope (Leica Microsystems, Wetzlar, Germany).[24]

Periodic Acid-Schiff (PAS) Staining

The intestinal mucosal barrier was evaluated using a PAS staining kit (Beyotime, China) according to the manufacturer's protocol. Briefly, paraffin-embedded sections were deparaffinized and rehydrated through graded alcohols. The sections were then oxidized with periodic acid solution, stained with Schiff's reagent, and counterstained with hematoxylin. After standard dehydration and mounting procedures, mucin-producing goblet cells were examined under a light microscope (Leica Microsystems, Germany).

Immunofluorescence (IF) Staining

Colon tissue sections were antigen-recovered with 0.01M citrate-EDTA antigen retrieval buffer (Biyuntian, P0086, diluted 1:50) by microwaving and then allowed to cool naturally. After incubation with hydrogen peroxide solution at 37°C for 10 minutes, the sections were blocked with 5% BSA (Biyuntian, ST023) for 30 minutes. The sections were then incubated with ZO-1 (Servicebio, GB111402, diluted 1:500, China) and Occludin (Servicebio, GB111401, diluted 1:500, China) overnight at 4°C. After washing with PBS, the sections were incubated with Alexa Fluor 488 (Servicebio, GB25303, diluted 1:500, China) and Coralite594 (Proteintech, SA00013-3-100, diluted 1:300, China). Finally, images were captured using an inverted fluorescence microscope (Leica Microsystems, Wetzlar, Germany).

Real-Time Quantitative Reverse Transcription PCR (RT-qPCR)

Total RNA was isolated from colon tissues using the TransZol Up Plus RNA Kit (TransGen Biotech, ER501-01, China) according to the manufacturer's protocol. cDNA was synthesized from 1 μg total RNA using the GoScript™ Reverse Transcription System (Promega, A5001, USA). RT-qPCR amplification was performed with the MonAmp™ ChemoHS qPCR Mix (Monad, MQ00401S, China). All experiments were conducted following the manufacturers' instructions. Primer sequences were listed in Table 1.

Western Blotting Assay

Colon tissues were weighed and homogenized in protein lysis buffer (1:6, w/v) using a tissue homogenizer. The homogenate was incubated on ice for 30 min with vortexing every 10 min, followed by centrifugation at 12,000 × g for 30 min at 4°C. The supernatant was collected, and protein concentration was determined using the BCA assay.

Table 1 Primers Employed for RT-qPCR Evaluations

Gene	Forward Primer	Reverse Primer
TLR-2	TCACTGGCAGGAGATGTGT	TGCTGAAGAGGACTGTTATGG
TLR-4	TTTCACCTGATGCTTCTTGCT	TCCTTACCCAGTCCTCATCCT
TLR-5	TCCTGACCAGAGCACATTTGCC	CCTTCAGTGTCCCAAACAGTCG
NLRP3	ATTACCCGCCCGAGAAAGG	TCGCAGCAAAGATCCACACAG
GSDMD-N	CCATCGGCCTTTGAGAAAGTG	ACACATGAATAACGGGGTTTCC
Caspase-1	AATACAACCACTCGTACACGTC	AGCTCCAACCCTCGGAGAAA
IL-1β	AAATGCCACCTTTTGACAGTGATG	GCTCTTGTTGATGTGCTGCTG
IL-18	GTGAACCCCAGACCAGACTG	CCTGGAACACGTTTCTGAAAGA
GAPDH	AGGTCGGTGTGAACGGATTTG	TGTAGACCATGTAGTTGAGGTCA

https://doi.org/10.2147/JIR.S533936

Aliquots were stored at −80°C for subsequent analysis. Protein samples were separated by SDS-PAGE and transferred onto PVDF membranes. After blocking with 5% skim milk in TBST, the membranes were incubated overnight at 4°C with primary antibodies against TLR4 (Proteintech, 19811-1-AP, 1:2000) and GSDMD-N (Affinity, DF13758, 1:1000). Following TBST washes, the membranes were incubated with HRP-conjugated secondary antibodies at 37°C for 2 h with gentle shaking. Protein bands were visualized using Western Lightning™ Chemiluminescence Reagent and captured on X-ray film. Quantitative analysis was performed using ImageJ software, with β-actin serving as the internal control for normalization.

Pharmacochemistry Analysis

Sample Preparation

Allow the decoction before concentration to settle overnight at 4°C, and then collect the supernatant. Metabolite were extracted with 50% methanol Buffer. Briefly, 20 μL of sample was extracted with 120 μL of precooled 50% methanol, vortexed for 1 min, and incubated at room temperature for 10 min; the extraction mixture was then stored overnight at -20°C. After centrifugation at 4,000 g for 20 min, the supernatants were transferred into new 96-well plates. The samples were stored at -80°C prior to the LC-MS analysis. In addition, pooled QC samples were also prepared by combining 10 μL of each extraction mixture.

Liquid Phase Parameters

All samples were acquired by the LC-MS system followed machine orders. Firstly, all chromatographic separations were performed using an ultra performance liquid chromatography (UPLC) system (SCIEX, UK). An ACQUITY UPLC T3 column (100mm*2.1mm, 1.8μm, Waters, UK) was used for the reversed phase separation. The column oven was maintained at 35°C. The flow rate was 0.4 mL/min and the mobile phase consisted of solvent A (water, 0.1% formic acid) and solvent B (Acetonitrile, 0.1% formic acid). Gradient elution conditions were set as follows: 0~0.5 min, 5% B; 0.50~7 min, 5% to 100% B; 70~8 min, 100% B; 80~8.1 min, 100% to 5% B; 8.10~10 min, 5%B. The injection volume for each sample was 4 μL.

Mass Spectrometry Parameters

A high-resolution tandem mass spectrometer TripleTOF5600plus (SCIEX, UK) was used to detect metabolites eluted form the column. The Q-TOF was operated in both positive and negative ion modes. The curtain gas was set 30 PSI, Ion source gas1 was set 60 PSI, Ion source gas2 was set 60 PSI, and an interface heater temperature was 650 °C. For positive ion mode, the Ionspray voltage floating were set at 5000 V, respectively. For negative ion mode, the Ionspray voltage floating were set at 4500V, respectively. The mass spectrometry data were acquired in IDA mode. The TOF mass range was from 60 to 1200 Da. The survey scans were acquired in 150 ms and as many as 12 product ion scans were collected if exceeding a threshold of 100 counts per second (counts/s) and with a 1+ charge-state. Total cycle time was fixed to 0.56 s. Four time bins were summed for each scan at a pulser frequency value of 11 kHz through monitoring of the 40 GHz multichannel TDC detector with four-anode/channel detection. Dynamic exclusion was set for 4 s. During the acquisition, the mass accuracy was calibrated every 20 samples. Furthermore, in order to evaluate the stability of the LC-MS during the whole acquisition, a quality control sample (Pool of all samples) was acquired after every 10 samples.

Network Pharmacology

Target Acquisition for XLAC

To identify bioactive compounds from the XLAC, the UPLC-Q-TOF-MS method was employed, successfully detecting a total of 460 compounds. Subsequently, a comprehensive list of XLAC related targets was obtained through collection, screening, and exclusion from PubChem database, Swiss target prediction database, and UniProt database for subsequent analysis.

Acquisition of Disease-Related Targets

With "UC" as the disease term, disease-related target was obtained from GeneCards database, OMIM database,

DisGenNET database, and Drugbank database. The Venny 2.1 platform was used to draw Venn maps to screen for common targets between herb target and disease target.

Constructing Protein-Protein Interaction (PPI) Networks

The potential action target was imported into the String platform (https://www.string-db.org/), with "Homo sapiens" set as the species and the minimum interaction score set to 0.4, hiding nodes without interaction links, and import the downloaded TSV file into Cytoscape 3.8.2 software to obtain the protein-protein interaction (PPI) network diagram between the XLAC and UC.

Enrichment Analysis of GO Function and KEGG Pathways

To clarify the role of potential targets of the XLAC in gene functions and signaling pathways, the intersection target of the XLAC for UC was entered into the DAVID 6.8 platform (https://david.ncifcrf.gov/summary.jsp) for Gene Ontology (GO) functional analysis of the intersection target protein genes. Based on $P < 0.05$, the top 10 enrichment terms in biological processes, cellular components, and molecular functions were selected. KEGG pathway enrichment analysis was performed using the Metascape platform, and the related signaling pathways enriched from the intersection target was filtered by *P*-value to obtain the top 30 pathways.

Bioinformatics Analysis

To explore the gene expression patterns related to UC, we conducted a search in the Gene Expression Omnibus (GEO) database using "UC" as the query term. Our research enabled us to obtain the dataset GSE11223, which consists of 63 active UC patient samples and 69 healthy subject samples. Subsequently, our focus shifted to identifying genes associated with Toll like receptors(TLRs). We used "TLR1, TLR2, TLR4, TLR5, TLR6, and TLR10" as search queries to retrieve relevant gene information from two different disease gene databases, laying the foundation for our subsequent analysis.

Molecular Docking

Based on the results of network pharmacology, the top 5 core active components ranked by degree value were searched in the PubChem database (https://pubchem.ncbi.nlm.nih.gov/), and their 3D structure files were downloaded. The protein structure of TLR4 was searched in the PDB protein structure database (https://www.rcsb.org/), and its protein structure file was downloaded. Molecular docking was performed using the CB-Dock2 platform (https://cadd.labshare.cn/cb-dock2/php/index.php), and the binding situation between active components and target proteins was understood based on the minimum Vina scores, with lower values indicating tighter binding. Docking scores less than −5 were considered significant, representing the docking scores of compounds and proteins. The ggplot software package was used to complete the information display, depicting the best docking images of receptors and ligands after visualization. Finally, we validated the screened targets through animal experiment.

Statistical Analysis

Data were expressed as mean ± SD. All statistical analyses and graphing were performed using SPSS 26.0 (SPSS, Armonk, United States) and GraphPad Prism 8.0.2 (GraphPad, San Diego, United States). One-way ANOVA was used to determine differences between groups, and results were considered statistically significant if the *P* value was less than 0.05.

Results

Beneficial Effect of XLAC on Intestinal Inflammation in UC Mice

The beneficial effect of XLAC on intestinal inflammation was determined in a mouse model of DSS-induced colitis (Figure 1A). 50 C57BL/6J male mice were divided into 5 groups, with 10 mice in each group. The results showed that mice in the Control group were in good spirits, active, had shiny and bright fur, were responsive, gained weight steadily, and had black-brown pellet-shaped feces. Mice in the Model group were listless, unresponsive, had rough and brittle fur,

lost weight, had foul-smelling perianal areas, and sticky bloody stools. Mice in the XLAC-H group and SASP group recovered well in terms of spirit, activity gradually returned, fur gradually became shiny and smooth, feces gradually formed, and occasionally had perianal contamination. Mice in the XLAC-L group were listless, had rough and brittle fur with less luster, decreased activity, and loose stools, with no significant overall improvement. Compared to the Control group, the weight of mice in the other four groups decreased to varying degrees, with the most significant weight loss in the Model group ($P<0.001$). There was no significant difference between the XLAC-L group and the SASP group, the XLAC-H group's weight was closest to the Control group, but there was still a statistically significant difference (Figure 1B). In addition to weight loss, DSS can also cause diarrhea and bloody stools. These symptoms can be quantified using the DAI score. The results showed that compared to the control group, the model group had significantly higher scores, while the XLAC group could effectively reduce scores (Figure 1C). Compared to the Control group, the colon length of mice in the Model group was significantly shortened ($P<0.001$), and the colon length of the XLAC group, especially the XLAC-H group, was longer than that of the Model group ($P<0.001$) (Figure 1D–F). The splenic index of mice in the Model group was significantly higher than the other four groups. After treatment with XLAC, the splenic index in mice was alleviated, and the spleen weight tended towards that of the Control group, indicating that the XLAC can alleviate the inflammatory response of UC (Figure 1E–G). The result of HE staining showed that the intestinal tissue structure of mice in the Control group was intact, with tight arrangement of mucosal epithelial cells, normal crypt structure, and minimal or no inflammatory cell infiltration; mice in the Model group had ulcers in the intestinal tissue, with crypt and villus atrophy, and significant inflammatory cell infiltration; mice in the XLAC-H group had no ulcers in the intestinal mucosa, the crypt structure was basically restored, and inflammatory cell infiltration was significantly relieved; mice in the XLAC-L group and SASP group had no ulcers in the intestinal mucosa, partial restoration of crypt structure, and relief of inflammatory cell infiltration (Figure 1H).

Beneficial Effect of XLAC on Intestinal Barrier in UC Mice

Neutral mucins, typically secreted by colonic goblet cells, can be stained red by AB-PAS. In this study, intestinal tissues from the Control group exhibited sufficient mucus secretion with well-organized goblet cell arrangement, whereas the Model group demonstrated significant depletion of goblet cells and complete absence of the mucus layer. Notably, XLAC-H treatment effectively restored mucus production and normalized goblet cell architecture, approaching physiological levels. Both XLAC-L and SASP groups showed partial but significant amelioration of these pathological features (Figure 2A–D). Immunofluorescence analysis further corroborated these findings by revealing marked upregulation of tight junction proteins ZO-1 and Occludin in ileal tissues following XLAC administration (Figure 2B,C,E and F). Collectively, the AB-PAS staining and immunofluorescence results provide compelling evidence that XLAC treatment promotes intestinal barrier repair and maintains mucosal homeostasis through restoration of both the mucus layer and epithelial tight junction complexes.

Exploring the Mechanism of XLAC in Treating UC Based on Network Pharmacology

A total of 460 compounds of XLAC were identified by UPLC-Q-TOF-MS (Figure 3A). There were 239 cross targets were obtained between the drug targets of XLAC and the disease targets of UC (Figure 3B). The 239 potential targets were imported into the STRING platform to construct a PPI network diagram of XLAC and UC (Figure 3C). Among the potential targets, inflammatory cytokine related indicators account for the majority. According to the degree values, PIK3R1, PIK3CA, MAPK3 and TLR4 were prominently displayed. TLR4, acting downstream of PIK3R1, PIK3CA, and MAPK3, is a key receptor in the inflammatory response and plays a crucial role in UC.[25,26] To further elucidate the potential target and biological function of XLAC, GO and KEGG pathway analyses were performed. GO enrichment analysis revealed that multiple genes may cooperatively exert biological effects. The molecular functions of XLAC in UC intervention primarily included kinase activity and protein kinase activity, while the biological processes involved hormone response, cellular response to nitrogen compounds, and positive regulation of response to external stimuli (Figure 3D). KEGG pathway analysis demonstrated that the targets were mainly enriched in inflammation-related pathways and signal transduction. Notably, the key inflammatory pathways included: Chemokine signaling pathway, Toll-like receptor signaling pathway, T-cell receptor signaling pathway, C-type lectin receptor signaling pathway, and Fc epsilon RI signaling pathway (Figure 3E). These findings suggest that the therapeutic effects of XLAC formula are predominantly mediated through the suppression of inflammatory responses.

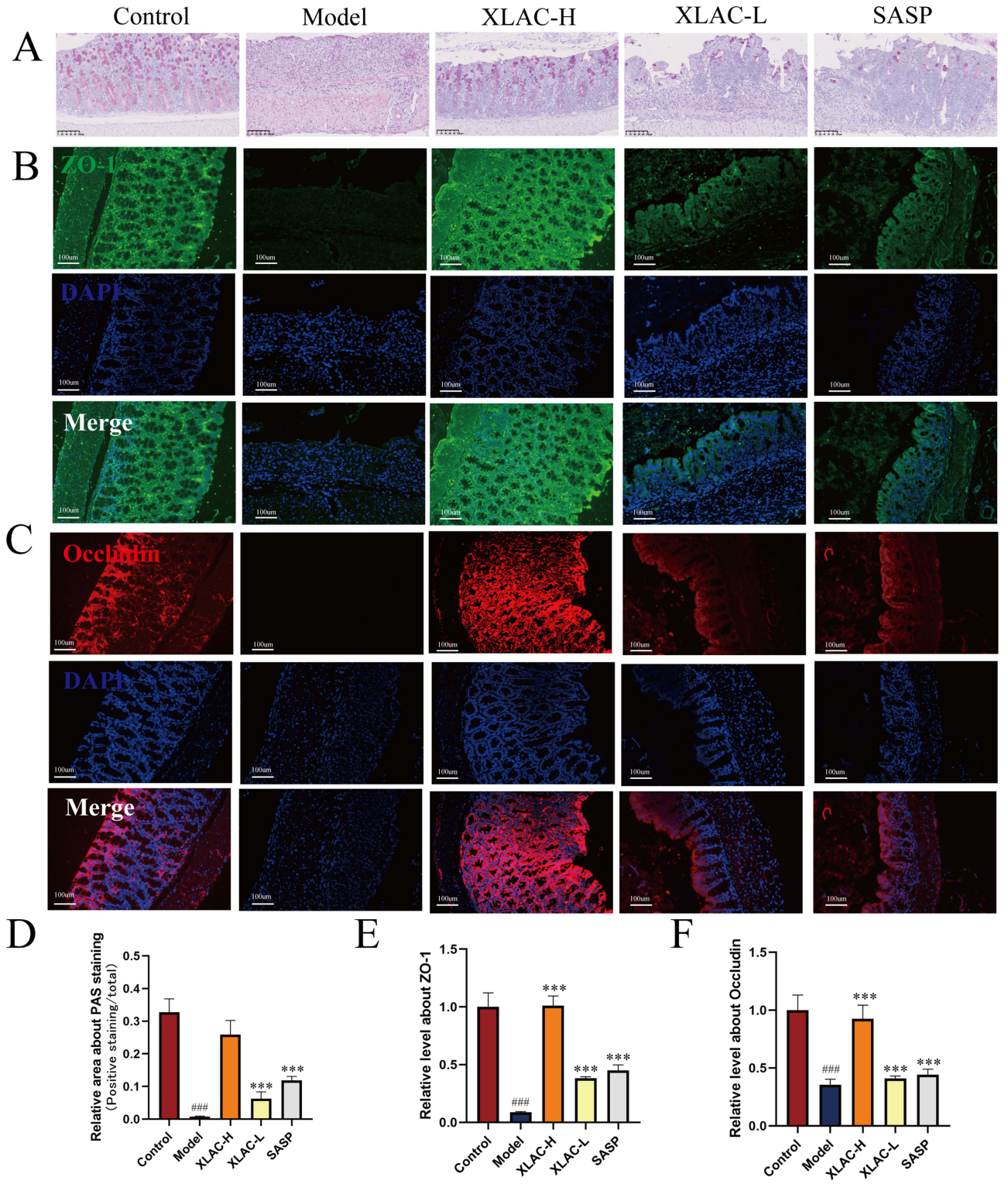

Figure 2 Beneficial effect of XLAC on intestinal inflammation in UC Mice. (**A**) Representative images of PAS staining for each group. (**B**) Representative images of IF staining about ZO-1 for each group. (**C**) Representative images of IF staining about Occludin for each group. (**D**) Statistical analysis result of PAS staining. (**E**) Statistical analysis result of IF staining for ZO-1. (**F**) Statistical analysis result of IF staining for Occludin. The data were denoted as the mean ± SD (n = 3). ###*P*<0.001, compared to Control group; ***P<0.001, compared to Model group.

https://doi.org/10.2147/JIR.S533936

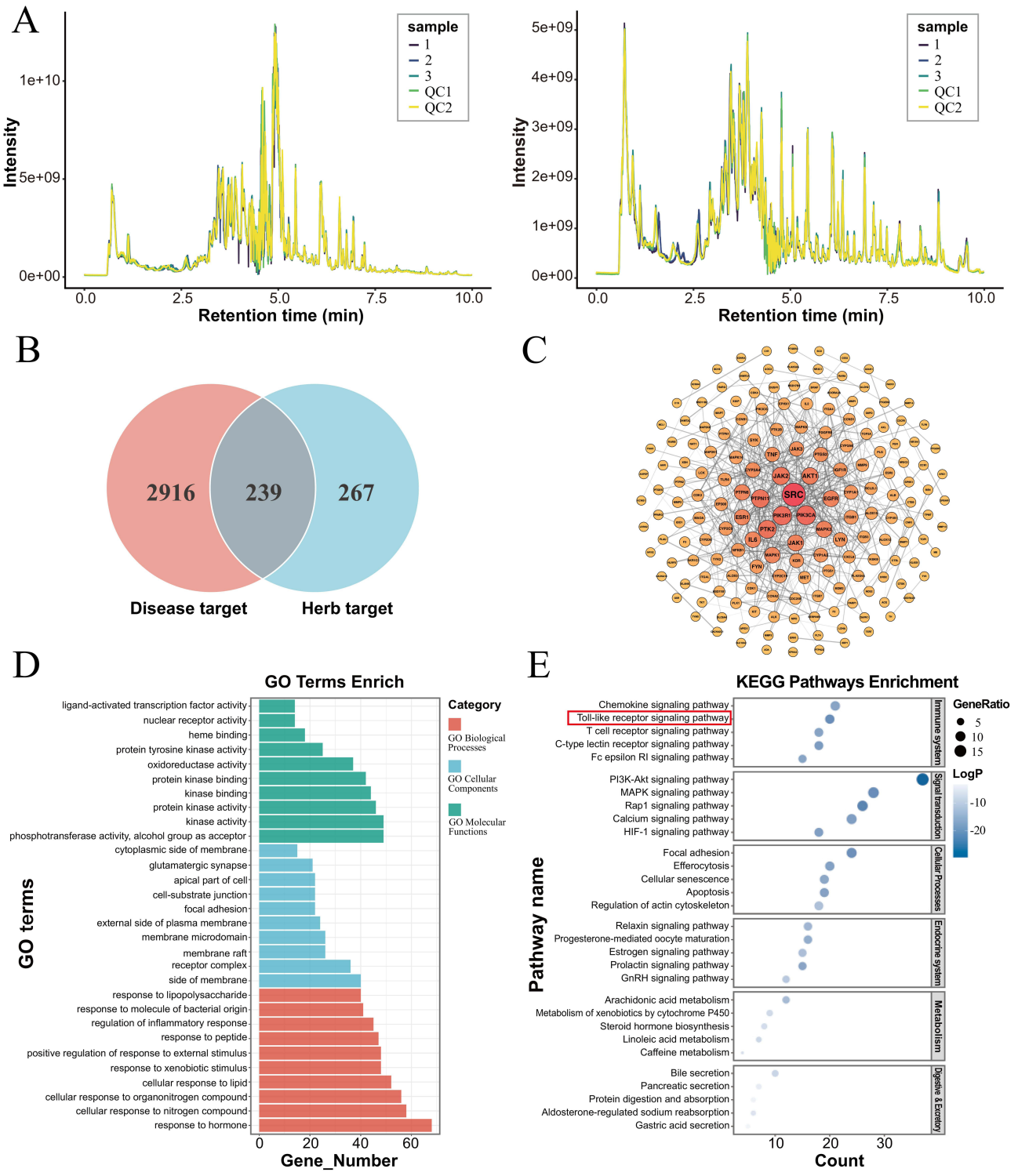

Figure 3 The network pharmacology analysis of XLAC in the treatment of UC. (**A**) Total ion chromatography of XLAC. (**B**) The Venn diagram of XLAC-UC relevant targets. There were 3,155 disease targets and 506 drug targets identified, with 239 overlapping targets between them. (**C**) PPI network construction of common genes. (**D**) The result of GO analysis. (**E**) The result of KEGG enrichment analysis.

Bioinformatics Reveals Key Role of TLR4 in the Mechanism of UC

This study focused on TLRs to identify key therapeutic target of XLAC in UC treatment. First, we analyzed the expression level of TLR1, TLR2, TLR4, TLR5, TLR6, and TLR10 in UC using the GSE11223 dataset. The results demonstrated that compared with the normal controls, the intestinal epithelium of UC patients exhibited significantly

upregulated expression of TLR2, TLR4, and TLR5 (P<0.05), suggesting their potential involvement in UC pathogenesis (Figure 4A). Subsequently, RT-qPCR validation in UC mouse colon tissues confirmed elevated TLR4 expression compared to normal controls, which was effectively downregulated upon XLAC treatment. In conclusion, our integrated bioinformatics and experimental approach identified TLR4 as a critical mediator underlying the therapeutic effects of XLAC in UC (Figure 4B).

Result of Molecular Docking

In the molecular docking experiment, we evaluated the binding interactions between active components and target proteins based on the minimum Vina scores, where lower values indicate stronger binding affinity. A docking score threshold of <-5 was set to define significant binding activity, representing the interaction strength between compounds and proteins (Figure 5D). Visualization of the optimal receptor-ligand docking conformations was performed using the ggplot software package (Figure 5A–C). The results demonstrated that TLR4 exhibits favorable binding affinity with key components in XLAC, including trans-4-coumaric acid, methyl cinnamate, and 2-furanylmethyl butanoate. These findings suggested that XLAC may exert its therapeutic effects through TLR4-related signaling pathway.

The Molecular Mechanism of XLAC in Treating UC by Acting on TLR4

RT-qPCR examination revealed that compared to the Control group, the expression of TLR4 of Model group mice was significantly increased ($P<0.001$), and treatment with XLAC could effectively reduce the expression of TLR4 (Figure 6A). The same results were also found in NLRP3 and GSDMD-N (Figure 6B and C). WB detection found that compared to the Control group, the protein expression of TLR4, NLRP3 and GSDMD-N in the colon tissue of the Model group was significantly increased ($P<0.001$); compared to the Model group, the XLAC treatment group significantly reduced the protein levels of TLR4, and GSDMD-N in the colon of UC mice in a dose-dependent manner ($P<0.05$) (Figure 6D and E). RT-qPCR detection found that the expression of caspase-1, IL-1β and IL-18 mRNA, related to pyroptosis, was significantly increased in the model group, and the expression levels were reduced after treatment with XLAC ($P<0.001$), indicating that XLAC can exert a therapeutic effect by inhibiting TLR4-mediated pyroptosis (Figure 6F–H).

Discussion

The complex pathology of UC makes it a difficult disease to control, not only stubborn and hard to heal, characterized not only by refractory inflammation but also by an increased risk of malignant tumors in patients with prolonged disease duration, ultimately endangering their health and survival.[27,28] XLAC, a traditional Chinese medicine formula developed under the guidance of traditional Chinese medicine theory, can significantly alleviate the main clinical manifestations of UC patients, such as bloody stools, abdominal pain, diarrhea, and weight loss. Our in vivo study results indicate that XLAC treatment significantly counteracted these adverse reactions, improving mucosal inflammation and bleeding. As shown by the various results, the DAI scores, weight, colon length, and spleen size of mice after traditional Chinese medicine intervention approached those of healthy controls. However, how XLAC affects the molecular mechanisms of UC remains unclear, which provides the motivation for this study. This study used network pharmacology experimental validation to confirm the relevant proteins and signaling pathways of XLAC intervention in UC.

In this study, the therapeutic effect of XLAC on UC was replicated through animal experiment. Subsequently, the compounds that actually exert the therapeutic effect of XLAC were identified through LC-MS/MS. Furthermore, network pharmacology predicted XLAC's primary targets in UC treatment, including PIK3R1, PIK3CA, AKT, and MAPK3—key regulators of inflammatory cytokine secretion, autophagy, and oxidative stress. Specifically, the activation of the PI3K family can lead to the secretion of inflammatory factors TNF-α and IL-1, and cell apoptosis, which are related to inflammatory diseases.[29] AKT, a downstream effector of PI3K, modulates cellular functions critical to inflammation progression.[30] Similarly, MAPK3, a member of the MAPK family, regulates inflammatory cytokine expression and cell proliferation upon activation by cytokines or microbial stimuli.[31] Collectively, the above content suggested that XLAC treatment for UC is closely related to the suppression of inflammation.

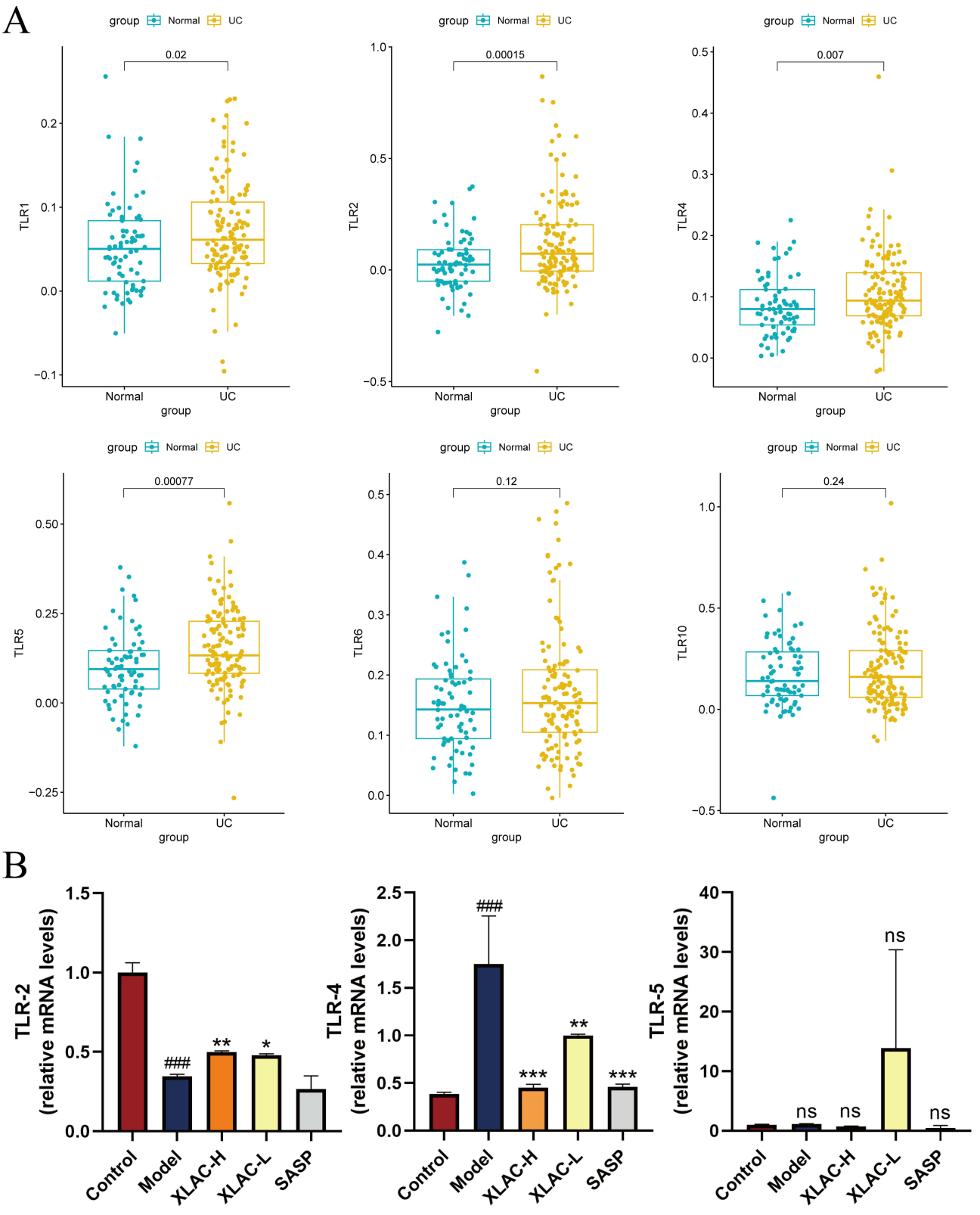

Figure 4 Bioinformatics analysis of UC targets. (**A**) Comparison results of TLRs based on bioinformatics analysis. (**B**) In vivo validation of TLRs. ###*P*<0.001, compared to Control group; The data were denoted as the mean ± SD (n = 3) *P<0.05,**P<0.01,***P<0.001, compared to Model group. ns represents no statistical difference.

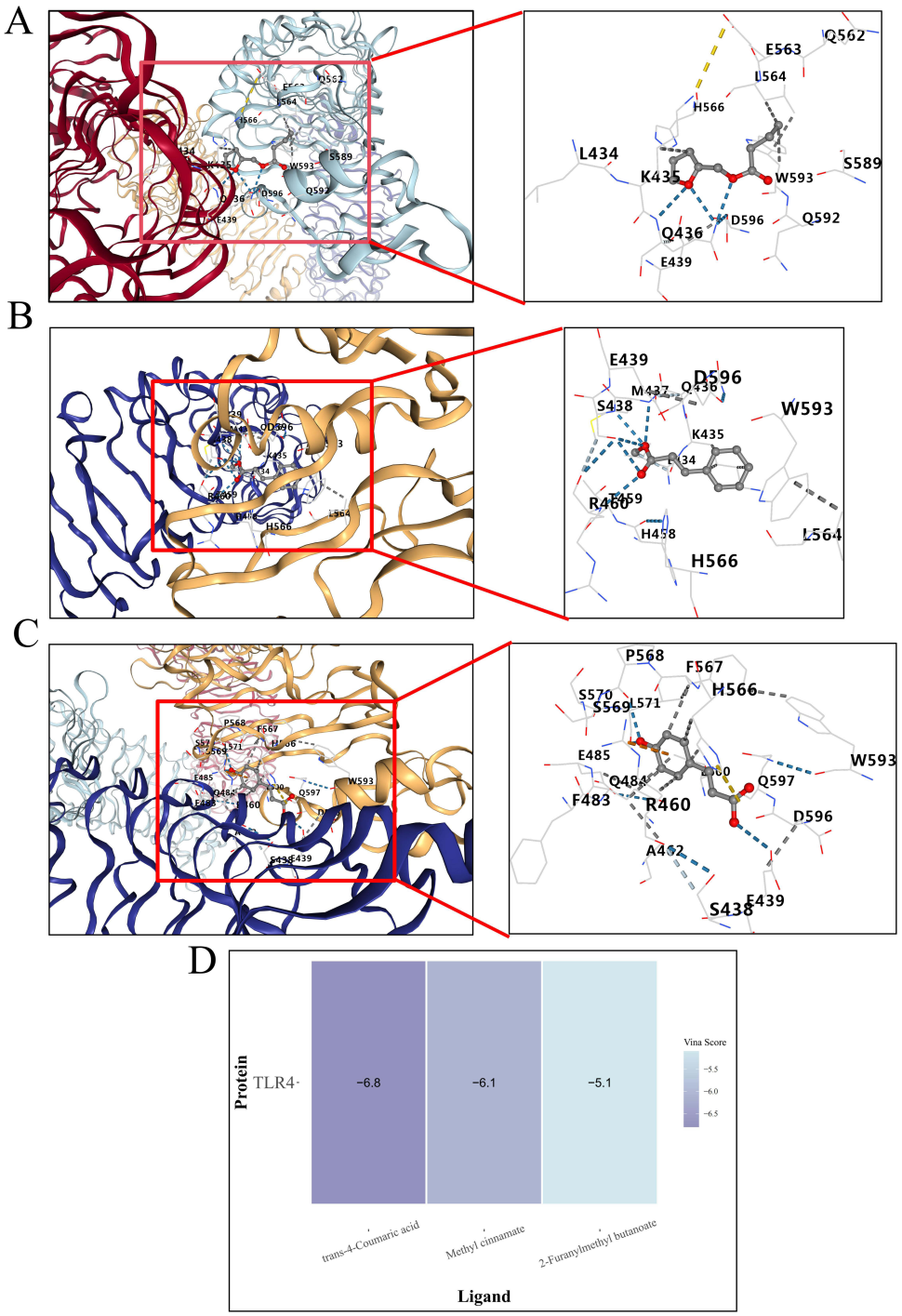

Figure 5 The docking results of three compounds with the central targets. (**A**) trans-4-coumaric acid with TLR4. (**B**) methyl cinnamate with TLR4. (**C**) 2-furanylmethyl butanoate with TLR4. (**D**) Score chart of molecular docking results. The data were denoted as the mean ± SD (n = 3).

Furthermore, KEGG pathway analysis indicated that XLAC potentially ameliorates UC through modulation of TLR signaling pathway. As critical components of innate immunity, TLRs serve as the first-line defense by recognizing both pathogen-associated molecular patterns (PAMPs) and damage-associated molecular patterns (DAMPs).[32] Studies have shown that TLRs expressed in the intestinal lamina propria have a regulatory effect on the inflammatory response.[33] Due to the large number of TLR family members, we initially analyzed the GEO clinical database and identified differentially expressed genes TLR2, TLR4, and TLR5, suggesting that these three may be involved in the pathogenesis of UC. To

https://doi.org/10.2147/JIR.S533936

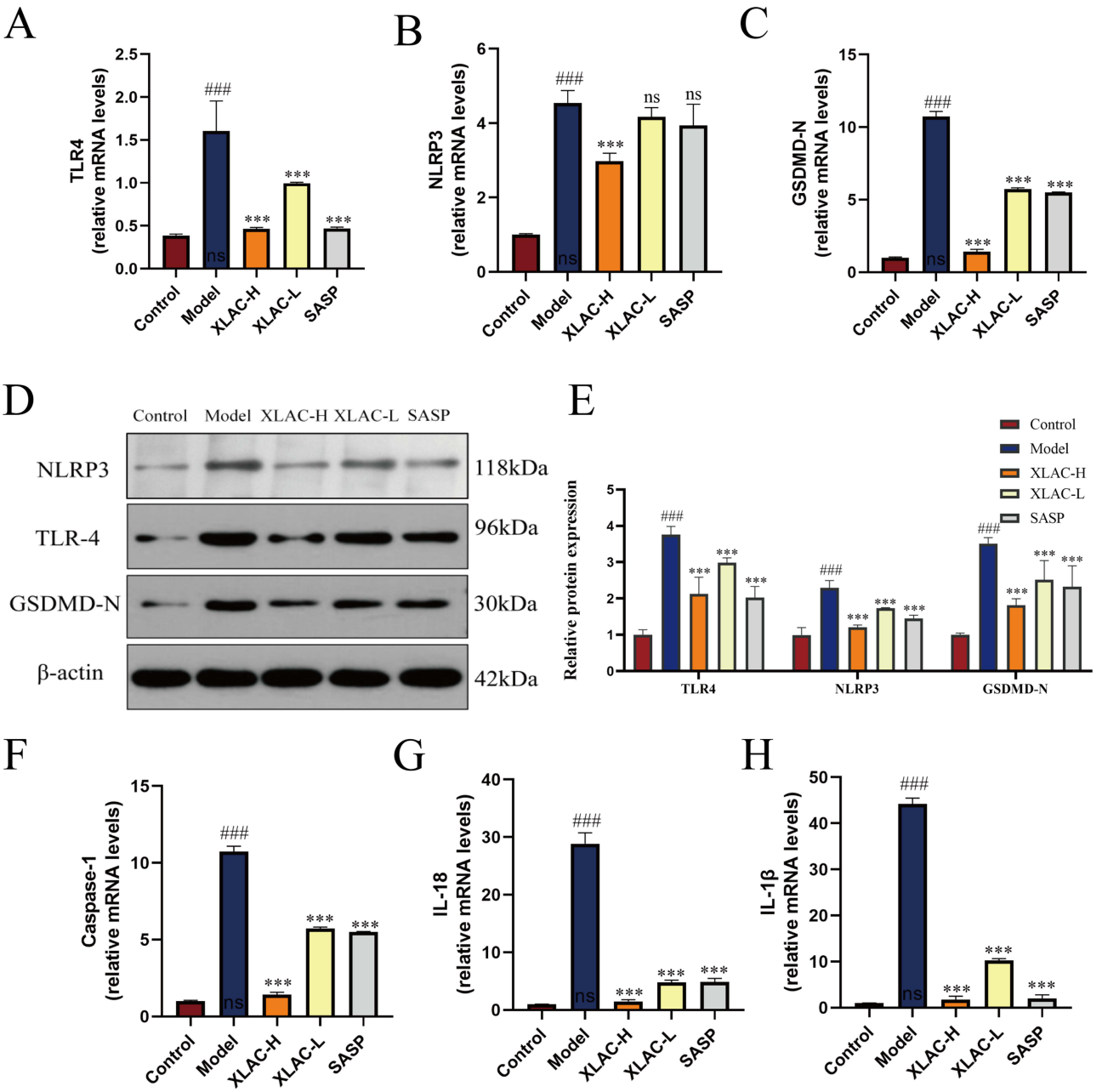

Figure 6 In Vivo Animal Experimental Validation. (**A**) The expression level about TLR4 of each group. (**B**) The expression level about NLRP3 of each group. (**C**) The expression level about GSDMD-N of each group. (**D**) Protein bands of TLR4, NLRP3 and GSDMD-N of each group assessed by Western blot. (**E**) Relative protein expression level of TLR4, NLRP3 and GSDMD-N of each group assessed by Western blot. (**F**) The expression level about Caspase-1 of each group was detected by qPCR. (**G**)The expression level about IL-18 of each group was detected by qPCR. (**H**) The expression level about IL-1β of each group was detected by qPCR. The data were denoted as the mean ± SD (n = 3) $^{###}P<0.001$, compared to Control group; $^{***}P<0.001$,compared to Model group. ns represents no statistical difference.

further clarify the specific therapeutic targets of XLAC, we subsequently performed qPCR validation and found that TLR4 mRNA expression was significantly upregulated in the Model group and showed sensitivity to XLAC treatment. Ultimately, molecular docking experiments demonstrated that TLR4 may exhibit strong binding affinity with key components in the drug-containing serum (such as trans-4-coumaric acid, methyl cinnamate, and 2-furanylmethyl butanoate). These results indicated that TLR4 serves as a crucial target through which XLAC exerts its regulatory effects on UC.

TLR4, as a membrane-bound pattern recognition receptor, serves as the critical "priming signal" for inflammasome activation.NOD-like receptor pyrin domain-containing protein 3 (NLRP3) is a type of intracellular pattern recognition

receptor that responds to pathogen-associated and damage-associated stimuli, as well as other danger signals that disrupt cellular homeostasis, and is involved in innate immune responses.[34] Under physiological conditions, NLRP3 and downstream IL-1β precursor and IL-18 precursor in cells are at very low levels to maintain a low-grade inflammatory state. However, the activation of the NLRP3 inflammasome can lead to excessive inflammatory responses, thereby promoting pathological processes and is related to a variety of human diseases, including type 2 diabetes, colitis, depression, and gout.[35] Previous studies have shown that the crosstalk between TLR4 and NLRP3 is evident in a variety of diseases, such as inflammatory bowel disease, Alzheimer's disease, and diabetic nephropathy, and the activation of TLR4 can affect the activation of the NLRP3 inflammasome through various pathways.[36–38] The activation of the inflammasome leads to the proteolytic activation of caspase-1, and GSDMD, as a direct downstream target of caspase-1, when cleaved by caspase-1, its N-terminal region translocates to the lipid membrane and oligomerizes to form pores with a diameter of about 10–14 nm, thus forming pores as pyroptosis effectors. These pores dissipate cellular ion gradients and allow water inflow, leading to cell swelling, osmotic lysis, and the release of intracellular inflammatory factors, such as IL-1β,and IL-18.[39] Network pharmacology and literature study only theoretically predict the therapeutic potential of XLAC in inhibiting pyroptosis through the TLR4/NLRP3/GSDMD pathway in UC, and the results of computational models are only referred to as "hypotheses" and need to be further verified by experiments. Therefore, experimental mouse models were used to verify these hypotheses. We used WB and RT-qPCR to assess the inhibitory effect of XLAC on pyroptosis and found that after Chinese medicine intervention, the protein of TLR4 and GSDMD-N in colon tissue was significantly reduced, and the mRNA of TLR4, NLRP3, caspase-1, and GSDMD was significantly decreased. We used RT-qPCR to assess the anti-inflammatory effect of XLAC and obtained encouraging data showing a reduction in pro-inflammatory cytokines (such as IL-18, IL-1β). In summary, the results of this study indicate that the abnormal activation of the TLR4/NLRP3/GSDMD signaling pathway leading to pyroptosis is an important mechanism of UC, and XLAC plays a therapeutic role by inhibiting this signaling pathway to alleviate pyroptosis. However, we need to further validate causal relationships using gene silencing or inhibitor models. Further standardization of herbal preparations is crucial for the clinical translation of this study.

Conclusion

In summary, our data indicate that XLAC acts on TLR4 to inhibit NLRP3-induced cell pyroptosis, alleviate inflammation, improve intestinal barrier function in UC mice, and act as an intestinal protectant. This discovery provides new and strong evidence for the efficacy of XLAC in the treatment of UC. While our findings strongly suggest that XLAC exerts therapeutic effects in UC by suppressing the TLR4/NLRP3/GSDMDmediated pyroptosis pathway, further studies using genetic or pharmacological inhibition models are warranted to confirm causality. Additionally, isolating and functionally validating the bioactive constituents of XLAC may facilitate the development of targeted therapies. These results lay the groundwork for the potential clinical application of XLAC or its components as adjunctive treatments in ulcerative colitis.

Abbreviations

DAMPs, damage-associated molecular patterns; ELISA, Enzyme-Linked Immunosorbent Assay; GO, Gene Ontology; GEO, Gene Expression Omnibus; H&E, Hematoxylin and Eosin Staining; IF, Immunofluorescence Staining; KEGG, Kyoto Encyclopedia of Genes and Genomes; NLRP3, NOD-like receptor pyrin domain-containing protein 3; PPI, protein-protein interactions; PAS, Periodic Acid-Schiff Staining; PAMPs, pathogen-associated molecular patterns; RT-qPCR, Quantitative Real-Time PCR; TCM, Traditional Chinese Medicine; UC, Ulcerative colitis; XLAC, Xianglian Anchang Decoction.

Data Sharing Statement

Data will be made available on request from the corresponding author [Shixiong Zhang].

Ethics Statement

All animal studies in this research were performed in accordance with the National Institutes of Health Guide for the Care and Use of Laboratory Animals and received approval from the Laboratory Animal Management Committee at Hebei University of Chinese Medicine (IACUC-HPHCM-2024078).

The GEO is a public database, and the patients included in this database have provided ethical approval for their data usage. Users can freely download relevant data for research purposes and publish related articles. Consequently, the Human Research Ethics Committee at Hebei University of Chinese Medicine has reviewed and waived the requirement for ethical approval for this study.

Acknowledgments

The authors gratefully acknowledge Lianchuan Biotechnology Co., Ltd. for their technical support, which significantly contributed to this research.

Author Contributions

All authors made a significant contribution to the work reported, whether that is in the conception, study design, execution, acquisition of data, analysis and interpretation, or in all these areas; took part in drafting, revising or critically reviewing the article; gave final approval of the version to be published; have agreed on the journal to which the article has been submitted; and agree to be accountable for all aspects of the work.

Funding

This work was supported by the Natural Science Foundation of Hebei Province of China under Grant No.H2025423083 (Youth Program) and the Natural Science Foundation of Beijing (No. 7232281) and the Scientific Research Plan Project of the Hebei Administration (No. 2022325).

Disclosure

The authors report no conflicts of interest in this work.

References

1. Le Berre C, Honap S, Peyrin-Biroulet L. Ulcerative colitis. *Lancet*. 2023;402(10401):571–584. doi:10.1016/S0140-6736(23)00966-2
2. Miyakita H, Yamamoto S, Uchino M, et al. Clinical features by disease duration in ulcerative colitis-associated cancers. *Colorectal Dis*. 2025;27(3):e70044. doi:10.1111/codi.70044
3. Piovani D, Hassan C, Repici A, et al. Risk of cancer in inflammatory bowel diseases: umbrella review and reanalysis of meta-analyses. *Gastroenterology*. 2022;163(3):671–684. doi:10.1053/j.gastro.2022.05.038
4. Narula N, Wong ECL, Dehghan M, et al. Association of ultra-processed food intake with risk of inflammatory bowel disease: prospective cohort study. *BMJ*. 2021;374:n1554.
5. Ananthakrishnan AN, Kaplan GG, Bernstein CN, et al. Lifestyle, behaviour, and environmental modification for the management of patients with inflammatory bowel diseases: an international organization for study of inflammatory bowel diseases consensus. *Lancet Gastroenterol Hepatol*. 2022;7(7):666–678. doi:10.1016/S2468-1253(22)00021-8
6. Chudy-Onwugaje KO, Christian KE, Farraye FA, Cross RK. A state-of-the-art review of new and emerging therapies for the treatment of IBD. *Inflamm Bowel Dis*. 2019;25(5):820–830. doi:10.1093/ibd/izy327
7. Liu Y, Li BG, Su YH, et al. Potential activity of traditional chinese medicine against ulcerative colitis: a review. *J Ethnopharmacol*. 2022;289:115084. doi:10.1016/j.jep.2022.115084
8. Li XV, Leonardi I, Putzel GG, et al. Immune regulation by fungal strain diversity in inflammatory bowel disease. *Nature*. 2022;603(7902):672–678.
9. Zu M, Liu G, Xu H, et al. Extracellular vesicles from nanomedicine-trained intestinal microbiota substitute for fecal microbiota transplant in treating ulcerative colitis. *Adv Mater*. 2024;36(41):e2409138. doi:10.1002/adma.202409138
10. Uzzan M, Martin JC, Mesin L, et al. Ulcerative colitis is characterized by a plasmablast-skewed humoral response associated with disease activity. *Nat Med*. 2022;28(4):766–779. doi:10.1038/s41591-022-01680-y
11. Tobi M, Antaki F, Rambus M, et al. Inflammatory bowel disease from the perspective of newer innate immune system biomarkers. *Gastrointest Disord*. 2025;7(1):22. doi:10.3390/gidisord7010022
12. van der Post S, Jabbar KS, Birchenough G, et al. Structural weakening of the colonic mucus barrier is an early event in ulcerative colitis pathogenesis. *Gut*. 2019;68(12):2142–2151. doi:10.1136/gutjnl-2018-317571
13. Bullard BM, McDonald SJ, Cardaci TD, et al. Panaxynol improves crypt and mucosal architecture, suppresses colitis-enriched microbes, and alters the immune response to mitigate colitis. *Am J Physiol Gastrointest Liver Physiol*. 2024;326(5):G591–G606. doi:10.1152/ajpgi.00004.2024

14. Kotla NG, Isa ILM, Rasala S, et al. Modulation of gut barrier functions in ulcerative colitis by hyaluronic acid system. *Adv Sci*. 2022;9(4): e2103189. doi:10.1002/advs.202103189
15. Mansouri P, Mansouri P, Behmard E, Najafipour S, Kouhpayeh A, Farjadfar A. Novel targets for mucosal healing in inflammatory bowel disease therapy. *Int Immunopharmacol*. 2025;144:113544. doi:10.1016/j.intimp.2024.113544
16. Dunleavy KA, Raffals LE, Camilleri M. Intestinal barrier dysfunction in inflammatory bowel disease: underpinning pathogenesis and therapeutics. *Dig Dis Sci*. 2023;68(12):4306–4320. doi:10.1007/s10620-023-08122-w
17. Patankar JV, Becker C. Cell death in the gut epithelium and implications for chronic inflammation. *Nat Rev Gastroenterol Hepatol*. 2020;17 (9):543–556. doi:10.1038/s41575-020-0326-4
18. Li W, Chen D, Zhu Y, et al. Alleviating pyroptosis of intestinal epithelial cells to restore mucosal integrity in ulcerative colitis by targeting delivery of 4-octyl-itaconate. *ACS Nano*. 2024;18(26):16658–16673. doi:10.1021/acsnano.4c01520
19. Burdette BE, Esparza AN, Zhu H, Wang S. Gasdermin D in pyroptosis. *Acta Pharm Sin B*. 2021;11(9):2768–2782. doi:10.1016/j.apsb.2021.02.006
20. Hadian K, Stockwell BR. The therapeutic potential of targeting regulated non-apoptotic cell death. *Nat Rev Drug Discov*. 2023;22(9):723–742. doi:10.1038/s41573-023-00749-8
21. Sun Y, Chan J, Bose K, Tam C. Simultaneous control of infection and inflammation with keratin-derived antibacterial peptides targeting TLRs and co-receptors. *Sci Transl Med*. 2023;15(686):eade2909. doi:10.1126/scitranslmed.ade2909
22. Vande Walle L, Lamkanfi M. Drugging the NLRP3 inflammasome: from signalling mechanisms to therapeutic targets. *Nat Rev Drug Discov*. 2024;23(1):43–66. doi:10.1038/s41573-023-00822-2
23. Wirtz S, Popp V, Kindermann M, et al. Chemically induced mouse models of acute and chronic intestinal inflammation. *Nat Protoc*. 2017;12 (7):1295–1309. doi:10.1038/nprot.2017.044
24. Jauregui-Amezaga A, Geerits A, Das Y, et al. A simplified geboes score for ulcerative colitis. *J Crohns Colitis*. 2017;11(3):305–313. doi:10.1093/ecco-jcc/jjw154
25. Shi YJ, Gong HF, Zhao QQ, Liu XS, Liu C, Wang H. Critical role of toll-like receptor 4 (TLR4) in dextran sulfate sodium (DSS)-Induced intestinal injury and repair. *Toxicol Lett*. 2019;315:23–30. doi:10.1016/j.toxlet.2019.08.012
26. Wang H, Zhou S, Zhang J, Lei S, Zhou J. Correlations between TLR polymorphisms and inflammatory bowel disease: a meta-analysis of 49 case-control studies. *Immunol Res*. 2019;67(1):142–150. doi:10.1007/s12026-018-9061-0
27. Kobayashi K, Toritani K, Kimura H, et al. Differences in prognosis and recurrence patterns between ulcerative colitis-associated colorectal cancer and sporadic colorectal cancer: a matched-pair analysis. *Ann Surg Oncol*. 2024;31(12):7807–7819. doi:10.1245/s10434-024-16158-z
28. Porter RJ, Kalla R, Ho GT, Sousa D. Ulcerative colitis: recent advances in the understanding of disease pathogenesis. *F1000Res*. 2020;9:9. doi:10.12688/f1000research.21431.1
29. Li H, Wen X, Ren Y, et al. Targeting PI3K family with small-molecule inhibitors in cancer therapy: current clinical status and future directions. *Mol Cancer*. 2024;23(1):164. doi:10.1186/s12943-024-02072-1
30. Khezri MR, Hsueh HY, Mohammadipanah S, Khalili Fard J, Ghasemnejad-Berenji M. The interplay between the PI3K/AKT pathway and circadian clock in physiologic and cancer-related pathologic conditions. *Cell Prolif*. 2024;57(7):e13608. doi:10.1111/cpr.13608
31. Bahar ME, Kim HJ, Kim DR. Targeting the RAS/RAF/MAPK pathway for cancer therapy: from mechanism to clinical studies. *Signal Transduct Target Ther*. 2023;8(1):455. doi:10.1038/s41392-023-01705-z
32. Fisch D, Zhang T, Sun H, et al. Molecular definition of the endogenous Toll-like receptor signalling pathways. *Nature*. 2024;631(8021):635–644.
33. Hackam DJ, Sodhi CP. Bench to bedside - new insights into the pathogenesis of necrotizing enterocolitis. *Nat Rev Gastroenterol Hepatol*. 2022;19 (7):468–479. doi:10.1038/s41575-022-00594-x
34. Liao Y, Kong Y, Chen H, Xia J, Zhao J, Zhou Y. Unraveling the priming phase of NLRP3 inflammasome activation: molecular insights and clinical relevance. *Int Immunopharmacol*. 2025;146:113821. doi:10.1016/j.intimp.2024.113821
35. Ye T, Tao WY, Chen XY, Jiang C, Di B, Xu LL. Mechanisms of NLRP3 inflammasome activation and the development of peptide inhibitors. *Cytokine Growth Factor Rev*. 2023;74:1–13. doi:10.1016/j.cytogfr.2023.09.007
36. Liu P, Zhang Z, Li Y. Relevance of the pyroptosis-related inflammasome pathway in the pathogenesis of diabetic kidney disease. *Front Immunol*. 2021;12:603416. doi:10.3389/fimmu.2021.603416
37. Xu L, Wang H, Yu QQ, et al. The monomer derivative of paeoniflorin inhibits macrophage pyroptosis via regulating TLR4/ NLRP3/ GSDMD signaling pathway in adjuvant arthritis rats. *Int Immunopharmacol*. 2021;101(Pt A):108169. doi:10.1016/j.intimp.2021.108169
38. Yang J, Wise L, Fukuchi KI. TLR4 cross-talk with NLRP3 inflammasome and complement signaling pathways in Alzheimer's disease. *Front Immunol*. 2020;11:724. doi:10.3389/fimmu.2020.00724
39. de Vasconcelos NM, Lamkanfi M. Recent insights on inflammasomes, gasdermin pores, and pyroptosis. *Cold Spring Harb Perspect Biol*. 2020;12 (5):a036392. doi:10.1101/cshperspect.a036392